Cold Flow Simulation of a 30 kW$_{th}$ CFB Riser with CPFD

D. Gündüz Raheem[1,2†], B. Yılmaz[1] and S. Özdoğan[1]

[1] *Marmara University, Institute of Pure and Applied Sciences, Kadikoy, Istanbul, 34722, Turkey*
[2] *Istanbul Medeniyet University, Faculty of Engineering and Natural Sciences, Dept. of Mechanical Engineering, North Campus, 34700, Uskudar, Istanbul, Turkey*

†*Corresponding Author Email: duygu.gunduz@medeniyet.edu.tr*

ABSTRACT

A 30 kW$_{th}$ Circulating fluidized bed (CFB) combustor is experimentally and numerically investigated under cold flow conditions. Barracuda software based on Computational Particle Fluid Dynamics (CPFD) method is utilized for simulations. The influences of bed inventory and drag model on flow hydrodynamics were investigated considering pressure and velocity profiles and particle concentration. Two advanced drag models, namely Energy minimization multi-scale (EMMS) and Wen-Yu/Ergun were selected for this study. The simulations were performed with initial bed material masses of 3.79, 4.55 and 5.20 kg corresponding to 2.5, 3 and 3.5 diameters height of riser, respectively. With increasing bed inventory pressure drops and solid concentration increase. The axial particle velocities slightly change with bed inventory. The comparison of simulation results with experimental measurements was resulted in good agreement (<5%) with both models. The simulation with EMMS drag model predicted the pressure profiles more accurately than Wen-Yu/Ergun drag model. The profiles of particle volume fraction and axial velocity demonstrate that core-annulus flow pattern was captured by both models. But EMMS drag model was better in revealing the meso-scale structures at instantaneous particle concentration distribution. Moreover, the influence of particle size distribution on particle volume fraction and particle velocity profiles is also investigated with two drag models.

Keywords: CFB; Experimental; Cold flow; CPFD; Drag model.

NOMENCLATURE

C_d	drag coefficient		np	number of particles per average unit volume
d	riser inner diameter		P	pressure
D_p	drag function		Re	Reynolds number
f_e	coefficient for EMMS drag law		z	axial height
F	drag force		β	constant in Eq. (6)
g	gravity		ρ	density
m	mass		τ_p	interparticle stress
m_p	initial bed mass		ω	coeficient for EMMS drag law

1. INTRODUCTION

The CFB technology is extensively used in gas-solid interacting thermolysis processes including combustion, oxy-combustion, gasification and catalytic cracking. Among the advantages of CFB technology are fuel adaptability, low pollutant emissions and high heat and mass transfer rates (Kunii, 1980). High particle concentration and intense gas-solid interactions are the main key features of CFB. Fluid Dynamics parameters affecting the system performance are important for the scaling, laying out and operation improvement of the CFB system (Thapa *et al.,* 2016). Several experimental studies are conducted to understand the complex hydrodynamics in CFB (Issangya *et al.,* 2000; Malcus *et al.,* 2000; Hu *et al.,* 2009; Lim *et al.,* 2012).

Experimental studies can present limited macro and local flow data, since it is not easy to study all parameters. Moreover, particularly for large capacity systems experimental methods are time consuming and costly. Computational Fluid Dynamics (CFD) modeling is an efficient and reliable approach to investigate the flow development in CFB systems with the great progress in computer science. Gas-solid hydrodynamics CFD models consist of two main techniques; Eulerian-

Eulerian (E-E) and Eulerian-Lagrangian (E-L) approaches. In the E-E approach, called Two Fluid Model (TFM) as well, the two phases are described as inter-penetrating fluids (Gidaspow, 1994). The equations of motion and continuity are solved for the fluid and particle phase (Hernández, 2008). The E-E approach has the advantage of lower computational cost, however, it predicts the flow characteristics of particles less accurately (Yeoh and Tu, 2009) due to the usage of single mean particle diameter rather than the particle size distribution (PSD). PSD has significant influences on the modelling results of CFB flow field. Therefore, continuity and momentum equations should consider a realistic particle size distribution rather than a specific particle size (Gidaspow, 1994).

On the contrary, the E-L approach using Discrete Element Method (DEM) considers particles individually. In this approach, for each individual particle the momentum equations are solved and interparticle collisions are also considered. By increasing the number of particles, simulations performed with Lagrangian methods become computationally more expensive. Thus, Lagrangian approach is limited to a relatively small particle numbers and two dimensional simulations (Taghipour *et al.,* 2005; Deen *et al.,* 2007).

The multi-phase particle-in-cell, namely MP-PIC, approach which uses E-L scheme is recently proposed due to the mentioned limitations of TFM and DEM (Andrews and ORourke, 1996; Snider, 2001). The fluid part is described as continuous phase however the particles are defined as Lagrangian computational particles having a particle size distribution (Snider, 2001) in the MP-PIC method. The continuous phase is modeled by Navier-Stokes equations, and the dynamics of the particle phase is modeled using the particle distribution function. The Lagrangian computational particles (called parcel) are not treated individually and they are assumed to have the same physical properties. Therefore, the large scale multiphase systems can be modelled by a comparatively small parcel numbers, that can reduce computational cost (Snider, 2007; Chen *et al.,* 2013).

The MP-PIC method was implemented to the simulations of multiphase and thermal reacting flows in fluidized bed (Li *et al.,* 2013; Berrouk *et al.,* 2017; Xie *et al.,* 2017). This approach has been utilized in several cold flow modeling studies including bubbling fluidized beds (Weber *et al.,* 2013; Liang *et al.* 2014; Fotovat *et al.,* 2015), risers of CFB's (Chen *et al.,* 2013; Shi *et al.,* 2014; Shi *et al.,* 2015a; Shi *et al.,* 2015b; Wang *et al.,* 2015) and full loop CFB systems (Wang *et al.,* 2014; Tu and Wang, 2018).

There is still limited experience to represent details of multiphase flows in CFB. Effects of some important modeling criteria such as computational particles number requirement, the chosen drag models and the bed inventory have not been fully understood yet.

In the two phase flows, the drag force controls the particle movement in the riser of a CFB system. Thus, the precision of the simulation depends highly on correct drag force prediction (Nikolopoulos *et al.,* 2013). The drag force is solved using drag models in the utilized software. One of the conventional drag models is the Wen-Yu/Ergun model which is widely used in dense flows. EMMS drag model which takes meso-scale forms in the CFB riser into account and considers heterogeneous characteristics of the flow (Chen *et al.,* 2016; Qi *et al.,* 2007) is recently preferred. EMMS drag model is often utilized with two-fluid model (TFM) in literature (Zhang *et al.,* 2008; Zhang *et al.,* 2010; Song *et al.,* 2014; Zeneli *et al.,* 2015; Qiu *et al.,* 2017). The CPFD approach which is based on MP-PIC method appears more cost-effective and efficient than TFM. In this study, EMMS drag model is utilized with CPFD approach for simulation of hydrodynamics of a CFB system.

Modelling hydrodynamics of fluidized bed systems under cold flow conditions is crucial to understand flow field characteristics. The developed flow field inside the CFB system influences the characteristics of the reactive systems significantly. Therefore, accurate prediction of solid-solid and solid-gas interactions for different operating conditions should be obtained using advanced models.

In the present work, a 30 kW$_{th}$ CFB combustor is investigated using the CPFD method under cold flow conditions. The cold flow experiments were conducted at TUBITAK Marmara Research Center facilities. In the numerical part, the same geometry is utilized for simulations. The three dimensional flow field is solved for transient conditions. Three different bed inventories are investigated with two drag models (Wen-Yu/Ergun and EMMS). The results are compared to available measurements. The hydrodynamics of the CFB system is examined in terms of distributions of pressure, velocity and solid concentration along the riser.

2. MODEL DESCRIPTION

2.1 Governing Equations

The MP-PIC approach solves the gas phase using Eulerian grids whereas the solid phase is accounted as Lagrangian particles. In this method, the motion of gas flow is determined by solving the Navier-Stokes equations which include a coupling between two phases by interphase drag force (Andrews and ORourke, 1996; Snider, 2001). Newton's second law of motion is utilized to define the particles motion.

The gas phase continuity equation is

$$\frac{\partial \theta_g \rho_g}{\partial t} + \nabla \left(\theta_g \rho_g \boldsymbol{u}_g \right) = 0 \qquad (1)$$

where u_g, ρ_g and θ_g represent the velocity, density and volume fraction of the gas, respectively.

The gas phase momentum equation is written as

$$\frac{\partial \theta_g \boldsymbol{u}_g}{\partial t} + \nabla \left(\theta_g \boldsymbol{u}_g \boldsymbol{u}_g \right) = -\frac{1}{\rho_g} \nabla P - \frac{1}{\rho_g} F + \theta_g \boldsymbol{g}$$
$$+ \frac{1}{\rho_g} \nabla \tau \qquad (2)$$

where P, $\boldsymbol{g}$ and F represent gas pressure, the gravitational acceleration and the momentum exchange rate between two phases, respectively. The fluid is assumed to be incompressible and both phases are isothermal.

$$F = \iint fm \left[D_p \left(\boldsymbol{u}_g - \boldsymbol{u}_p \right) - \frac{1}{\rho_p} \nabla P \right] dm \, dv \qquad (3)$$

where $\boldsymbol{u}_p$ and ρ_p are the particle velocity and density. D_p is the drag function and f stands for probability distribution function obtained from Liouville equation.

The Lagrangian method is implemented to model particle motion with particle acceleration defined as

$$\frac{d\boldsymbol{u}_p}{dt} = D_p \left(\boldsymbol{u}_g - \boldsymbol{u}_p \right) - \frac{1}{\rho_p} \nabla P + g - \frac{1}{\theta_p \rho_p} \nabla \tau_p \quad (4)$$

The first term in the right hand side of Eq. (4) is acceleration and the second term is pressure gradient. The remaining terms are gravity and the inter-particle stress gradient, τ_p, respectively. The particle velocity is presented by

$$\frac{d\boldsymbol{x}_p}{dt} = \boldsymbol{u}_p \qquad (5)$$

where $\boldsymbol{x}_p$ is the location of particles.

In the present model, the spatial gradients are used to solve the particle-particle collisions then they are interpolated to each particle. The volume fraction of particles is computed from particle volume mapped to the grid. Then, the particle stress is derived from particle volume fraction. The normal stress of particle is expressed as (Snider, 2001)

$$\tau_p = \frac{P_s \theta_p{}^\beta}{max \left[\left(\theta_{cp} - \theta_p \right), \varepsilon \left(1 - \theta_p \right) \right]} \qquad (6)$$

where P_s represents a positive constant, θ_{cp} is the volume fraction of particle at the close packing limit. β is a constant ($2 < \beta < 5$). The constant ε is a number having the order of 10^{-7} to avoid the singularity at close packing (Snider, 2001).

2.2 Drag Models

In CPFD modeling of gas–solids flow, the selected drag model influences the simulation results significantly. Therefore, different drag models should be tested.

In this study, two drag models were used.

✓ Wen-Yu/Ergun (Gidaspow, 1994)

✓ EMMS (Yang *et al.,* 2003)

The drag force exerted on a particle is given as

$$\boldsymbol{F}_p = m_p D \left(\boldsymbol{u}_g - \boldsymbol{u}_p \right) \qquad (7)$$

where m_p and D represent the particle mass and the drag function, respectively. In most of the models, the drag function depends on flow conditions, geometry and the drag coefficient C_d.

The Wen-Yu model is suggested for the particle volume concentrations within the range of 0.01 to 0.61 (Wen and Yu, 1966) whereas the Ergun drag model is suitable for the range from 0.47 to 0.7 (Ergun, 1952). By combining of two mentioned drag models, Wen-Yu/Ergun model is obtained and recommended for dense particulate flows (Gidaspow, 1994).

The Wen-Yu/Ergun model is defined as in Table 1.

D_1 and D_2 are the Wen-Yu and Ergun drag functions, respectively. EMMS model is utilized to reveal the heterogeneous structure and capture the multiphase flow interactions in the dense region of CFB. The EMMS model is recommended for resolving the formation and breaking up of clusters (Chen *et al.,* 2013). The EMMS drag law is implemented in CPFD as in Table 1.

3. EXPERIMENTAL SETUP

Experimental measurements were conducted in a 30 kW$_{th}$ CFB system (Fig. 1) at TUBITAK-MRC premises.

The laboratory scale system contains a riser, a fuel feeding system, a return leg, cyclones, ash hoppers, primary air fan, ID fan and bag filter. The height of the CFB riser is 6 m with 0.108 m of the inner diameter.

The silica sand bed material was used having PSD given in Fig. 2. Its particle and bulk densities are determined to be 2650 kg/m^3 and 1530 kg/m^3 respectively. Inlet air velocity was set constant at 3 m/s. Pressures along the riser were measured with pressure transmitters which are placed at 0.32, 1.25, 2.248, 3.148, 4.036, 4.936, 5.84 m above the distributor plate. Three different particle masses were studied to observe the effect of solid bed inventory on the pressure distribution along the riser. Operating conditions and gas and particle properties used in measurements are listed in Table 2 in detail.

4. NUMERICAL SETUP

Barracuda® software using CPFD scheme is used in the simulations. In the model, the riser of the experimental system is analyzed. The particle phase is silica sand and air is defined as fluid phase in the model. For the initial conditions, three initial particle masses (m$_p$= 3.79, 4.55 and 5.20 kg) are set with PSD of Fig. 2 and air feeding is identical with experiments. Inlet and outlet boundary conditions are introduced as the same with experiments and their locations are shown in Fig. 3. The fluidization air is fed into system at the riser bottom with inlet velocity of 3 m/s; particles are recycled to the riser

Table 1 Drag Coefficients for Wen-Yu Ergun and EMMS Model

Wen-Yu/Ergun model	$C_d = \begin{cases} D_1 & \theta_p < 0.75\theta_{cp} \\ (D_2 - D_1)\dfrac{\theta_p - 0.75\theta_{cp}}{0.85\theta_{cp} - 0.75\theta_{cp}} & 0.75\theta_{cp} \geq \theta_p \geq 0.85\theta_{cp} \\ D_2 & \theta_p > 0.85\theta_{cp} \end{cases}$
EMMS model	$f_e = \begin{cases} \dfrac{1}{180\theta_p}\left(150\dfrac{\theta_p}{\theta_g} - 1.75Re\right) & \theta_g < 0.74 \\ \left(1 + 0.15\,Re^{0.678}\right)\omega & \theta_g \geq 0.74 \text{ and } Re < 1000 \\ 0.44\dfrac{Re}{24}\omega & \theta_g \geq 0.74 \text{ and } Re \geq 1000 \end{cases}$ $\omega = \begin{cases} -0.5760 + \dfrac{0.0214}{4(\theta_g - 0.7463)^2 + 0.0044} & 0.74 \leq \theta_g \leq 0.82 \\ -0.0101 + \dfrac{0.0038}{4(\theta_g - 0.7789)^2 + 0.0040} & 0.82 < \theta_g \leq 0.97 \text{ b} \\ -31.8295 + 32.895\theta_g & 0.97 < \theta_g \leq 1 \end{cases}$
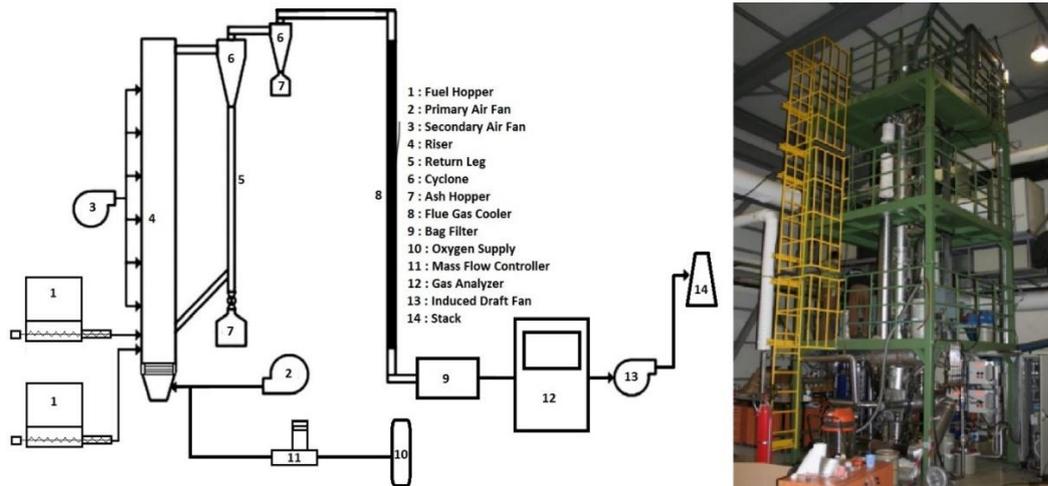
Fig. 1. 30kW$_{th}$ CFB Combustor (schematic diagram on the left, a photograph of the system on the right) (Kayahan and Ozdogan, 2016).

located 0.143 m above the distributor. Pressure boundary condition is implemented at the outlet. The other simulation parameters are given in Table 2.

4.1 Grid Test

A grid was generated for the geometry given in Fig. 3. A grid independency analysis was implemented to make sure that the grid size does not affect the simulation results. Four grid sizes were used with approximately 20k, 40k, 50k and 80k cells. In Fig. 4, the distribution of the time averaged axial pressure was used to examine the influences of the grid size.

The simulation results for the 40k, 50k and 80k cells grid sizes are in good agreement but the results of 20k cells grid size deviate and predict higher

pressure profile along the riser. The 40k cells grid size was chosen in simulations due to the computational cost without losing precision.

In Barracuda software, computational particles are defined as particle groups having the same physical properties. It is necessary to determine the computational particles number for CPFD calculations. Selection of this number affects the accuracy and computational efficiency of the simulations. For our study sensitivity analysis for computational particles number was done like grid sensitivity analysis. Five computational particles (parcel number) with 12084, 46464, 90288, 118772, 196040 which correspond to the particle numbers per average unit volume (np) value of 5, 20, 40, 60, 80, respectively, were tested (Fig. 5). The axial

pressure profile simulations with 12084 and 46464 parcel numbers are omitted due to their higher deviation rates compared to those with the 90288, 118772 and 196040 parcels. Therefore, 90288 parcel number is selected for the simulations to save the computational cost.
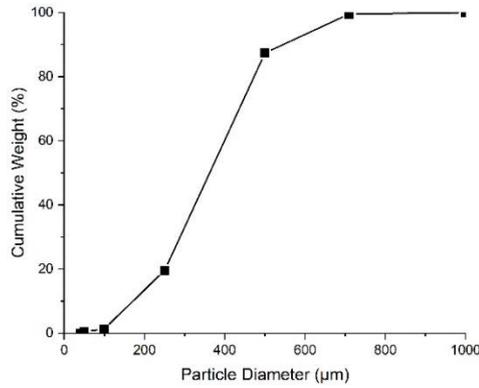
Fig. 2. Particle size distribution (PSD) of the silica sand.

Table 2 Experimental and simulation parameters

Parameter	Experimental	Simulation
Operating temperature (K)	298	298
Operating pressure (kPa)	101.325	101.325
Gas density (kg/m^3)	1.2	1.2
Gas viscosity (Pa.s)	1.9×10^{-5}	1.9×10^{-5}
Superficial gas velocity (m/s)	3	3
Particle density (kg/m^3)	2650	2650
Total bed inventory, M_P (kg)	3.79; 4.55; 5.20	3.79; 4.55; 5.20
Initial bed material height (m)	2.5d; 3d; 3.5d	2.5d; 3d; 3.5d
Particle-particle interaction		
Maximum momentum redirection from collision(%)	-	40
Close-pack particle volume fraction	-	0.58
Particle to wall interaction		
Normal-to-wall retention coefficient	-	0.3
Tangent-to-wall retention coefficient	-	0.99
Diffuse bounce	-	0
Time Control		
Initial time step (s)	-	0.001
Total time (s)	-	100
Start time for averaging (s)	-	20
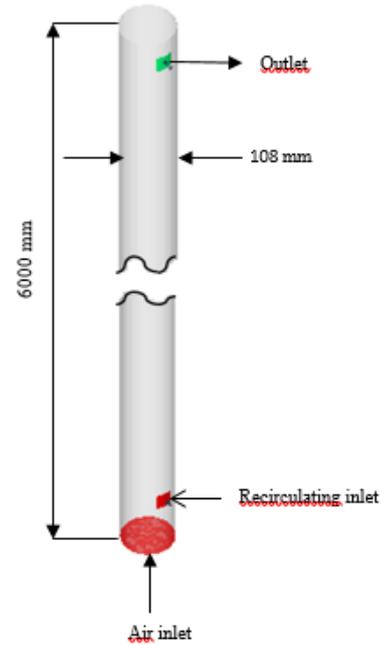
*d: Inner diameter of the riser
Fig. 3. Schematic diagram of the computational geometry.
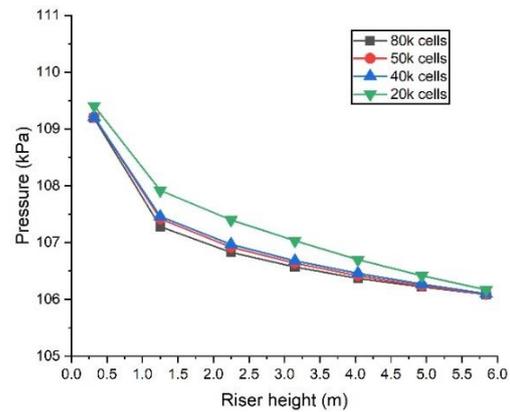
Fig. 4. Pressure distribution along the CFB riser for 4 grid sizes.
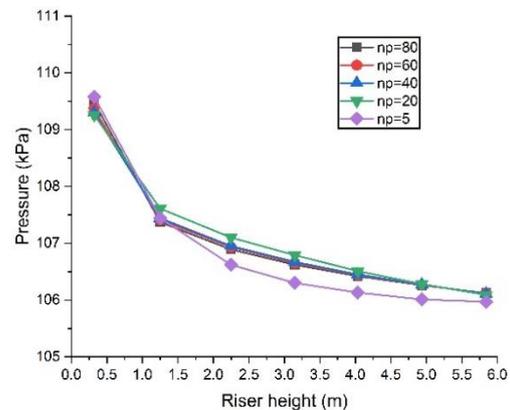
Fig. 5. Pressure distribution along the CFB riser for 5 parcel numbers.

5.   RESULTS AND DISCUSSION

5.1 The Effect of Solid Bed Inventory on Pressure Distribution

The solid bed inventory has an important influence on the pressure drops along the riser. The higher the solid bed mass, the greater the pressure drop (Li and Kwauk, 1980). Figures 6 and 7 present the experimental and simulation results with 2.5d, 3d and 3.5d static bed heights corresponding to 3.79, 4.55, and 5.20 kg bed material mass, respectively. The comparison of measured and computed time averaged pressure distributions along the riser for different bed inventories are illustrated in Fig. 6 with the Wen-Yu/Ergun Drag model and Fig. 7 with the EMMS model.

Both models predict higher pressure in the bottom section of the riser due to higher particle volume fractions parallel to experimental results.   The variation of static bed height affects the pressure distribution in the riser as seen in Figs. 6 and 7. It is revealed by both models that pressure drops significantly at the lower section of the riser due to higher concentration of particles for all bed inventories. Moreover, EMMS model results in higher decrease in pressure compared to Wen-Yu/Ergun model in that region. Then, the decrease in pressure is observed less at the upper section of the riser. Wen-Yu/Ergun model predicts pressure drop more however EMMS model computes a slight change in that region.
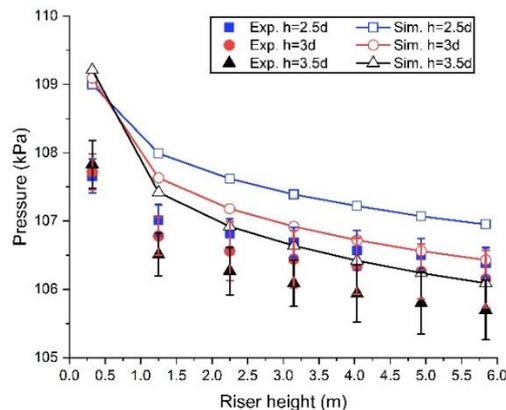
Fig. 6. Time averaged pressure distribution along the riser under different bed inventories (Wen-Yu/Ergun Drag model).

The expected increase in pressure drops with the increase of the total bed mass is observed with both the simulated and experimental results. It is seen that by increasing the bed inventory, pressure drop along the lower section of the riser increases both in experiments and simulations. For both drag models, comparisons of the measured and simulated pressure profiles along the riser show good agreement (Figs. 6 and 7). Calculation errors are reasonable and less than 5%. Both models slightly overestimate the pressure data. Wen Yu/Ergun model has better predicted qualitatively the correct decreasing trend. However, the EMMS based drag model predicts

better the pressure distribution quantitatively. Thus, EMMS model appears to predict the pressure profile along the riser more accurately.
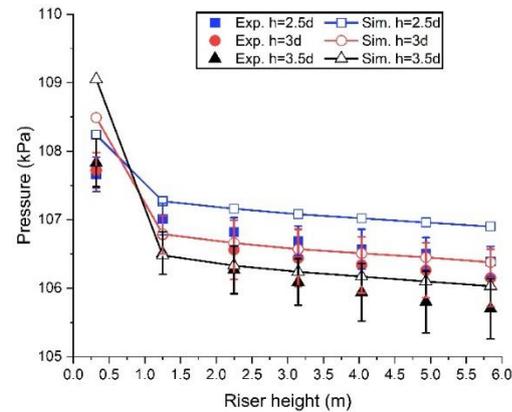
Fig. 7. Time averaged pressure distribution along the riser under different bed inventories (EMMS drag model).

5.2   The Effect of Solid Bed Inventory on Particle Volume Fraction Average particle volume fraction

A conventional CFB riser may be divided into two regions which are called core and annulus. The gas velocity is quite low sometimes even negative in the annulus whereas it is higher than the superficial velocity in the core. The solids move upwards and downwards through the bed within the clusters. Solids moving up through the core mostly drift sideways by cause of hydrodynamic interactions as they meet with gas velocities negative or too low to bring the clusters upwards. Therefore, the clusters begin to move downward in the annulus region (Arena *et al.*, 1988; Tung *et al.*, 1988; Werther, 2005). Additional complex interactions between wall and particles may lead solid movements downwards near the wall region as well (Wang *et al.*, 2015).

Figure 8 depicts the radial profiles of the time-averaged particle volume fraction at five locations in axial direction (z = 10d, 20d, 30d, 40d, 50d m) for different bed inventories by comparing the results of EMMS and the Wen-Yu/Ergun drag models. As it is seen from the figures; the axial particle volume fraction is higher at each axial position in the Wen-Yu/Ergun simulation than the corresponding data in the EMMS simulations. When the bed inventory increases, the concentration of particle also increases in the riser. Both models show the typical core-annulus flow especially at the dense region in the riser. The particle concentration changes from the axis to the wall and it is the highest near the wall and lowest along the axis of the riser. Wen-Yu/Ergun model shows a relatively more parabolic distribution while EMMS model predicts a slight change of particle concentration in the core region. The particle volume fraction decreases from bottom to upper regions and its profile is found much flatter in the upstream region of the riser due to more homogeneous flow in that region.
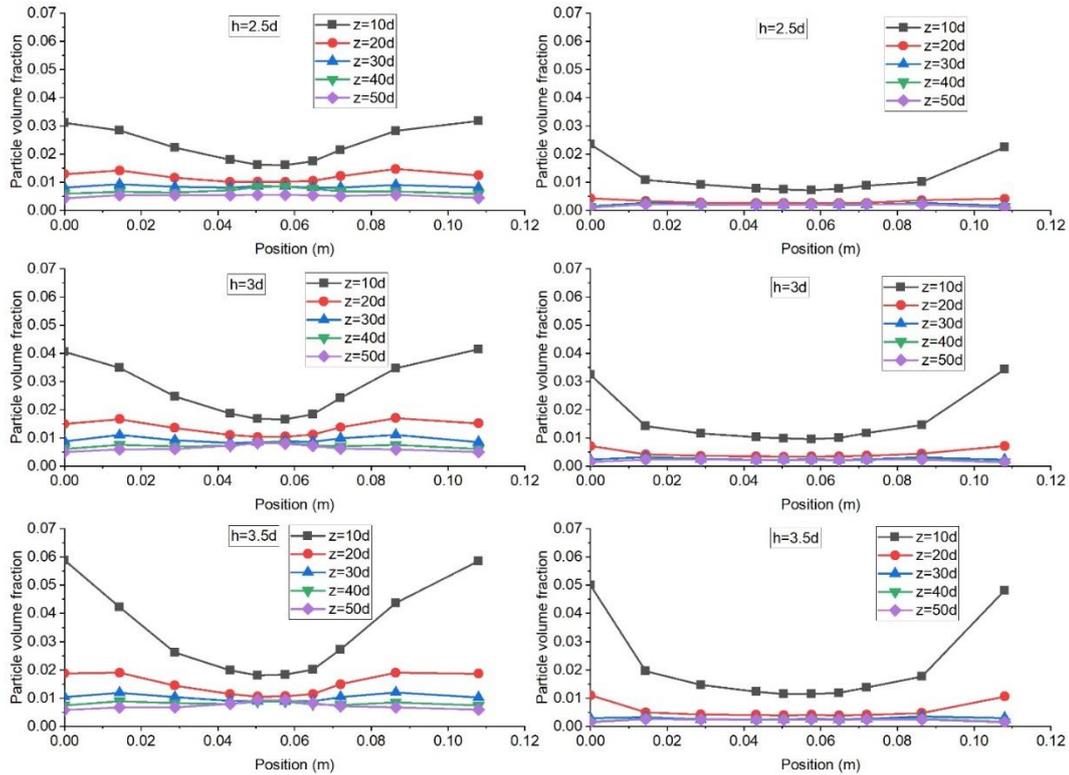
Fig. 8. Average particle volume fraction under different bed inventories, a) Wen-Yu/Ergun based, left column b) EMMS based, right column Instantaneous particle volume fraction.

Figure 9 illustrates the distribution of instantaneous particle volume fraction for the bed inventory height of 3d using Wen-Yu/Ergun and EMMS models, and five axial heights (z=10d, 20d, 30d, 40d, 50d). This figure indicates that solid concentration is more close to the wall region in line with the averaged results of Fig. 8. In the simulation results with the EMMS model, the particle volume fraction shows non-uniform characteristics at each axial heights and particle clusters appear mostly near the wall area. However, in the Wen-Yu/Ergun simulation, particle distribution is nearly uniform axially without clusters presence and region separation. In the literature (Wang *et al.,* 2008; Li *et al.,* 2012; Chen *et al.,* 2013), it is reported that EMMS drag model considers the heterogeneous configuration (i.e. cluster formation) in the CFB risers. Thus, it gives more precise results compared to homogeneous drag models (i.e. Wen-Yu/Ergun drag model).

5.3 The Effect of Solid Bed Inventory on Particle Velocity Distribution.

The axial particle velocity profiles in radial direction for different bed inventories at five different heights in the riser for both drag models are given in Fig. 10. Both models have predicted lower or even negative axial solid particles velocities near the wall, while the particle velocity is upward and reaches a maximum in the core region. It indicates that back mixing occurs and core-annulus flow structure is predicted (Yang *et al.,* 2003). In the Wen-Yu/Ergun model particle velocities in the core region decreases regularly in the axial direction and

becomes nearly flat in upper region of the riser. Moreover, it predicts particle velocities larger than that found by EMMS drag model. In the simulations, near-wall effects and core annulus flow pattern are correctly estimated at each height with both drag models. Differently from Wen-Yu/Ergun model, in the simulation with EMMS drag model, particle velocity distribution shows slightly the 'M' shaped profile as monitored by (Yang *et al.,* 2004; Nikolopoulos *et al.,* 2010; Wang and Liu, 2010). As shown in Figure 10, solid bed inventory appears to have a more profound effect on particle velocities in the simulation with Wen-Yu/Ergun model compared to the EMMS simulation. Wen-Yu/Ergun drag model gives slightly higher velocities at higher solid inventories however EMMS model finds almost no change.

5.4 The Effect of PSD on Flow Dynamics

CPFD approach has the capability of working with the particle size distribution for gas-solid flow modeling. In previous sections, the simulations were performed with a PSD shown in Fig. 2. In order to examine the effect of PSD on gas particle flow dynamics an average particle diameter case has been studied as in literature (Chen *et al.,* 2013; Wang *et al.,* 2014). The surface volume average particle diameter was used in simulations equal to 0.301mm.

The computed radial profiles of time-averaged particle volume fraction with and without PSD at three locations in axial direction (z =10d, 20d, 30d), where variations are high, for the bed inventory
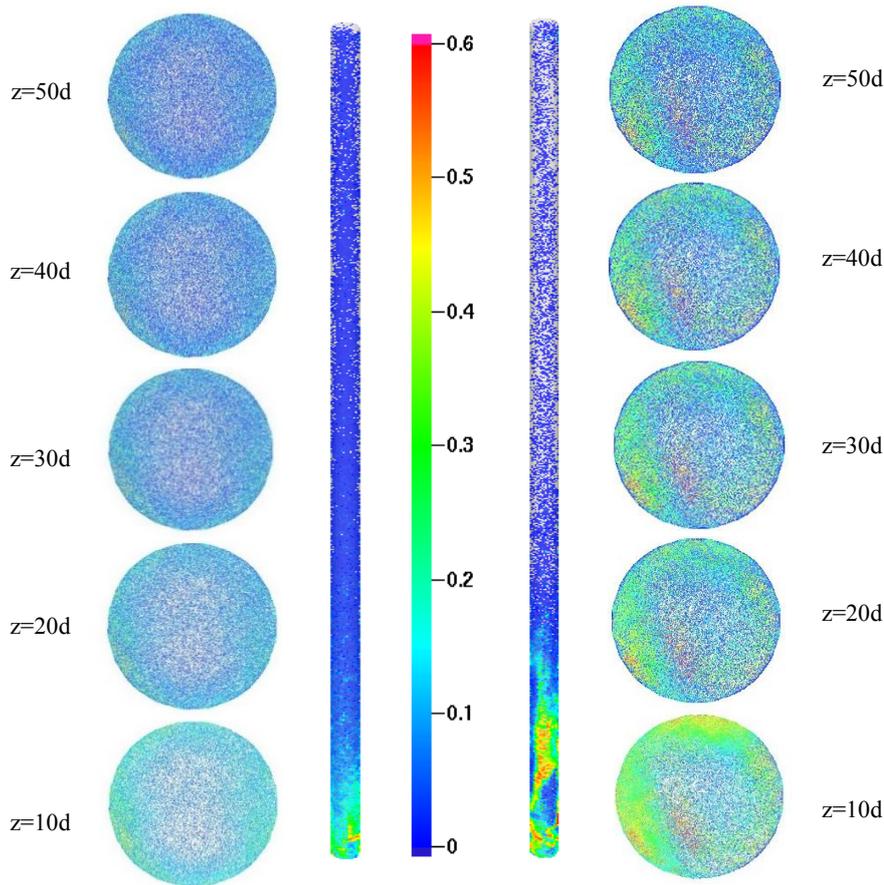
Fig. **9. Instantaneous particle volume fraction for h=3d, a) Wen-Yu/Ergun based on the left, b) EMMS based on the right.**

height of 3d are shown in Figs. 11a and b. The results of Wen-Yu Ergun model and EMMS model are shown in Figs. 11a and 11b, respectively. The axial particle volume fraction is found higher at each axial position in the Wen-Yu/Ergun simulation than the EMMS simulations in line with the simulation results of Fig. 8.

The PSD affects the averaged particle volume fraction at the lower section of the riser (z=10d) significantly while it has limited influence at the upper sections of the riser predicted by the Wen-Yu Ergun model simulations. In addition, the particle volume fraction augmented highly near the wall while it decreased slightly in the core region at lower section of the riser since the number of large particles with PSD case is comparatively less than averaged particle diameter case. The particle volume fraction is found higher in the upper sections of the riser with PSD since the small-diameter particles can move freely and accumulate in those regions. In the EMMS model, small difference is observed between particle volume fractions simulated using the average particle size and that with the PSD as seen in Fig. 11b.

Figure 12 presents the axial particle velocity profiles in radial direction for average particle size at three different heights in the riser for both drag models. Particle velocities in the simulation with Wen-

Yu/Ergun model are higher compared to the EMMS simulations and found large at the lower section with both models in line with the results in Fig. 10. Axial particle velocity is also negative near the wall and increases towards the center due to back mixing. It is seen that the velocity profiles become flatter with average particle diameter cases for all locations in axial direction in Wen-Yu Ergun model. Moreover, average particle velocities are obtained higher with PSD case. Slight differences are observed between the time-averaged axial solid velocity profiles with EMMS model simulated with the average particle diameter and the PSD case.

CONCLUSION

The cold flow model simulations of the 30 kW$_{th}$ CFB combustor with CPFD showed good agreement with measured data.

The investigation of the effects of bed inventory and drag model on flow characteristics considering pressure profile, particle concentration and velocity profile with EMMS and Wen-Yu/Ergun drag models have led to the following conclusions in terms of simulations.

The simulated pressure profiles with both drag models resulted in accordance with available measurements along the riser. Both models slightly
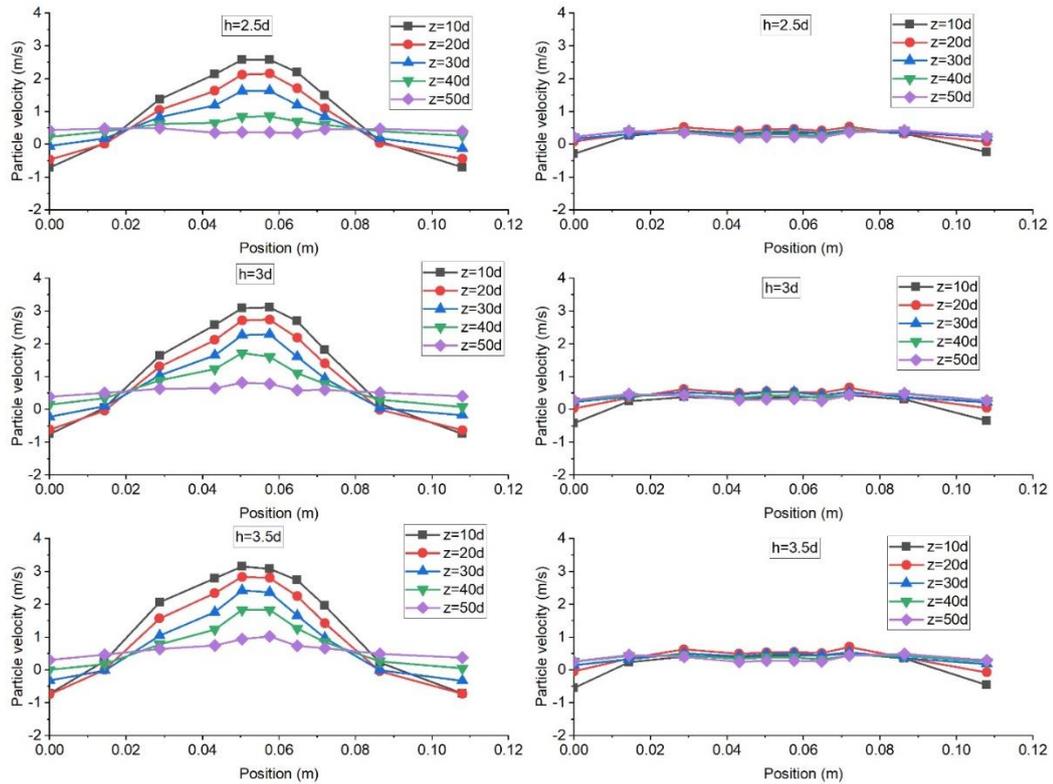
Fig. 10. Average solid axial velocity distribution under different bed inventories, a) Wen-Yu/Ergun based, left column b) EMMS based, right column.
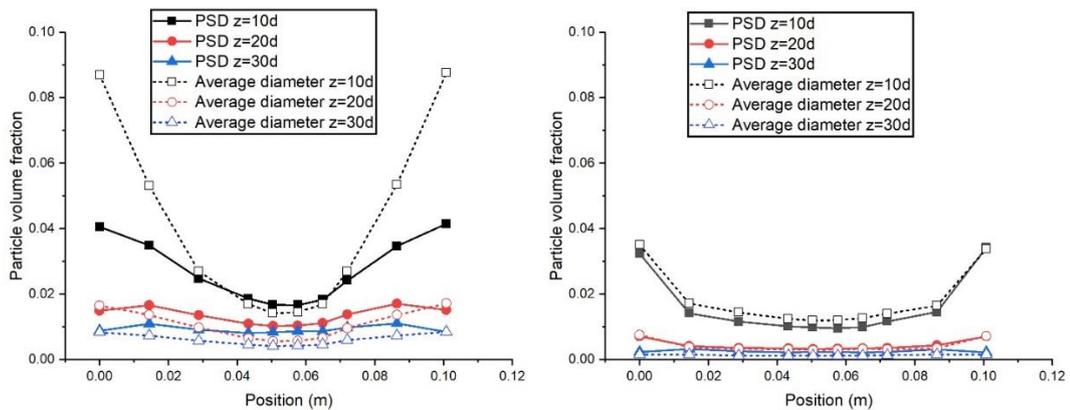
Fig. 11. Average particle volume fraction with and without PSD for h=3d, a) Wen-Yu/Ergun based, left column b) EMMS based, right column.
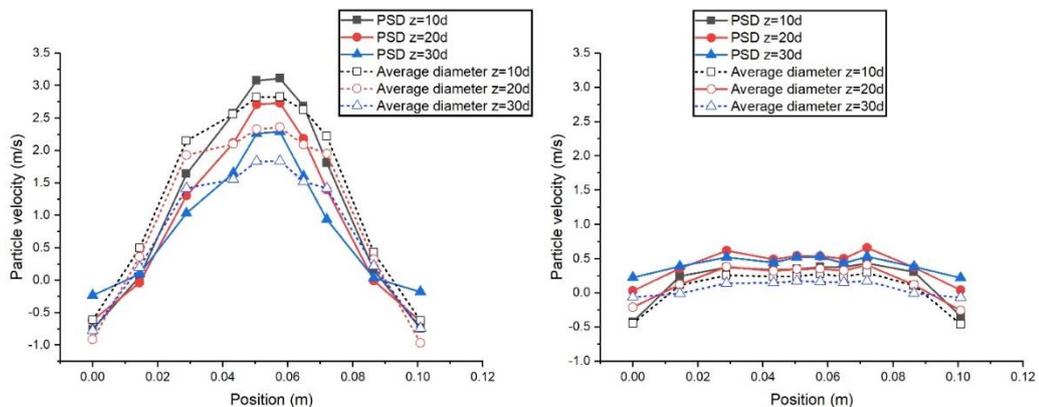
Fig. 12. Average solid axial velocity distribution with and without PSD for h=3d, a) Wen-Yu/Ergun based, left column b) EMMS based, right column.

overestimate the pressure data with errors less than %5. Wen-Yu/Ergun model has better predicted qualitatively the correct decreasing pressure trend. However, the EMMS based drag model shows better prediction in the pressure distribution of the CFB riser quantitatively. Thus, EMMS model appears to predict the pressure profile more precise.

In simulations with both drag models it is found that volume fraction of particles increases as the bed inventory increases. Whereas it decreases along the riser.

The core annulus structure has captured by both drag models, particularly at the dense particle region. Simulation with EMMS model considers heterogeneous characteristics (cluster formation) better than Wen-Yu/Ergun model.

The solid axial velocities slightly increase as the bed inventory increases in both drag models. Wen-Yu/Ergun model predicts one core annulus flow pattern. However, EMMS drag model shows M shaped profile as reported by (Yang *et al.,* 2004; Nikolopoulos *et al.,* 2010; Wang and Liu, 2010).

The influence of PSD is observed more in particle volume fraction distributions with Wen-Yu Ergun model. Utilizing a PSD has significantly decreased the particle volume fraction especially at the lower section of the riser. The effect of PSD cannot be captured well by EMMS model.

In the present study, it is found that the CPFD approach is a promising tool and predicts flow hydrodynamics accurately.

ACKNOWLEDGMENTS

REFERENCES

Andrews, M. J. and P. J. O'Rourke (1996). The multiphase particle-in-cell (MP-PIC) method for dense particulate flows. *Int. J. Multiphase Flow* 22(2), 379-402.

Arena, U., A. Cammarota, L. Massimilla and P. Pirozzi (1988). The hydrodynamics behavior of two circulating fluidized bed units of different sizes, In *Circulating Fluidized Bed Technology II, Basu, P., Large, J. F. (Eds.)*, Pergamon Press, Oxford, pp. 223-229.

Berrouk, A. S., C. Pornsilph, S. S. Bale, Y. Du and K. Nandakumar (2017). Simulation of a Large-Scale FCC Riser Using a Combination of MP-PIC and Four-Lump Oil-Cracking Kinetic Models. *Energy Fuels* 31(5), 4758-4770.

Chen, C., J. Werther, S. Heinrich, H. Y. Qi and E. U. Hartge (2013). CPFD simulation of circulating fluidized bed risers. *Powder Technology* 235, 238-247.

Chen, C., Q. Dai and H. Y. Qi (2016). Improvement of EMMS drag model for heterogeneous gas-solid flows based on cluster modeling. *Chemical Engineering Science* 141, 8-16.

Deen, N. G., M. V. S. Annaland, M. A. V. D. Hoef and J. A. M. Kuipers (2007). Review of discrete particle modeling of fluidized beds. *Chemical Engineering Science* 62(1-2), 28-44.

Ergun, S. (1952). Fluid flow through packed columns. *Chemical Engineering Progress* 48, 89-94.

Fotovat, F., A. Abbasi, R. J. Spiteri, H. de Lasa and J. Chaouki (2015). A CPFD model for a bubbly biomass–sand fluidized bed. *Powder Technology* 275, 39-50.

Gidaspow, D. (1994). *Multiphase flow and fluidization: Continuum and kinetic theory descriptions* New York: Academic Press.

Hernández, J. L. (2008). *Influence of drag laws on segregation and bubbling behavior in gas-fluidized beds.* Ph.D. Dissertation, University of Colorado, USA.

Hu, N., H. Zhang, H. R. Yang, S. Yang, G. X. Yue, J. F. Lu and Q. Liu (2009). Effects of riser height and total solids inventory on the gas–solids in an ultra-tall CFB riser. *Powder Technology* 196, 8-13.

Issangya, A. S., J. R. Grace, D. R. Bai and J. X. Zhu (2000). Further measurement of flow dynamic in a high-density circulating fluidized bed riser. *Powder Technology* 111, 104-113.

Kayahan, U. and S. Ozdogan (2016). Oxygen enriched combustion and co-combustion of lignites and biomass in a 30 kW$_{th}$ circulating fluidized bed. *Energy* 116, 317-328

Kunii, D. (1980). Chemical reaction engineering and research and development of gas–solid system. *Chemical Engineering Science* 35, 1887-1911.

Li, F., F. Song, S. Benyahia, W. Wang and J. Li (2012). MP-PIC simulation of CFB riser with EMMS based drag model. *Chemical Engineering Science* 82, 104-113.

Li, T., K. Chaudhari, D. VanEssendelft, R. Turton, P. Nicoletti, M. Shahham and C. Guenther (2013). Computational Fluid Dynamic Simulations of a Pilot-Scale Transport Coal Gasifier: Evaluation of Reaction Kinetics. *Energy Fuels* 27, 7896-7904.

Li, Y. and M. Kwauk (1980). The dynamics of fast fluidization, in: *Grace, J., Matsen M. (Eds.), Fluidization, vol. III*, Plenum Press, New York, pp. 537–544.

Liang, Y., Y. Zhang, T. Li and C. Lu (2014). A critical validation study on CPFD model in simulating gas–solid bubbling fluidized beds. *Powder Technology* 263, 121-134.

Lim, M. T., S. Pang and J. Nijdam (2012).

Investigation of solids circulation in a cold model of a circulating fluidized bed. *Powder Technology* 226, 57-67.

Malcus, S., G. Chaplin and T. Pusley (2000). The hydrodynamics of the high-density bottom zone in a CFB riser analyzed by means of electrical capacitance tomography (ECT). *Chemical Engineering Science* 55, 4129–4138.

Nikolopoulos, A., K. Atsonios, N. Nikolopoulos, P. Grammelis and E. Kakaras (2010). An advanced EMMS scheme for the prediction of drag coefficient under a 1.2MWth CFBC isothermal flow-Part II: Numerical implementation. *Chemical Engineering Science* 65(13), 4089-4099.

Nikolopoulos, A., N. Nikolopoulos, A. Charitos, P. Grammelis, E. Kakaras, A. R. Bidwe and G. Varela (2013). High-resolution 3-D full-loop simulation of a CFB carbonator cold model. *Chemical Engineering Science* 90, 137-150.

Qi, H. Y., F. Li, B. Xi and C. You (2007). Modeling of drag with the Eulerian approach and EMMS theory for heterogeneous dense gas-solid two-phase flow. *Chemical Engineering Science* 62(6), 1670-1681.

Qiu, X. P., L. M. Wang, N. Yang and J. H. Li (2017). A simplified two-fluid model coupled with EMMS drag for gas-solid flows. *Powder Technology* 314, 299-314.

Shi, X., R. Sun, X. Lan, F. Liu, Y. Zhang and J. Gao (2015a). CPFD simulation of solids residence time and back-mixing in CFB risers. *Powder Technology* 271, 16-25.

Shi, X., X. Lan, F. Liu, Y. Zhang and J. Gao (2014). Effect of particle size distribution on hydrodynamics and solids back-mixing in CFB risers using CPFD simulation. *Powder Technology* 266, 135-143.

Shi, X., Y. Wu, X. Lan, F. Liu and J. Gao (2015b). Effects of the riser exit geometries on the hydrodynamics and solids back-mixing in CFB risers: 3D simulation using CPFD approach. *Powder Technology* 284, 130-142.

Snider, D. M. (2001). An incompressible three-dimensional multiphase particle-in- cell model for dense particle flows. *Journal of Computational Physics* 170, 523-549.

Snider, D. M. (2007). Three fundamental granular flow experiments and CPFD predictions. *Powder Technology* 176, 36-46.

Song, F. F., W. Wang, K. Hong and J. H. Li (2014). Unification of EMMS and TFM: structure-dependent analysis of mass, momentum and energy conservation. *Chemical Engineering Science* 120, 112-116.

Taghipour, F., N. Ellis and C. Wong (2005). Experimental and computational study of gas–solid fluidized bed hydrodynamics. *Chemical Engineering Science* 60, 6857-6867.

Thapa, R. K., A. Frohner, G. Tondl, C. Pfeifer and B. M. Halvorsen (2016). Circulating fluidized bed combustion reactor: Computational Particle Fluid Dynamic model validation and gas feed position optimization. *Computers and Chemical Engineering* 92, 180-188.

Tu, Q. and H. Wang (2018). CPFD study of a full-loop three-dimensional pilot-scale circulating fluidized bed based on EMMS drag model. *Powder Technology* 323, 534-547.

Tung, Y., J. Li and M. Kwauk (1988). Radial voidage profiles in a fast fluidized bed, In *Fluidization'88, Kwauk, M., Kunii, D. (Eds.),* Science Press, Beijing, pp. 139-145.

Wang, J. and Y. Liu (2010). EMMS-based Eulerian simulation on the hydrodynamics of a bubbling fluidized bed with FCC particles. *Powder Technology* 197, 241-246.

Wang, Q., H. Yang, P. Wang, J. Lu, Q. Liu and H. Zhang (2014). Application of CPFD method in the simulation of a circulating fluidized bed with a loop seal: Part I-Determination of modeling parameters. *Powder Technology* 253, 814-821.

Wang, Q., T. Niemi, J. Peltola, S. Kallio, H. Yang and J. Lu (2015). Particle size distribution in CPFD modeling of gas–solid flows in a CFB riser. *Particuology* 21, 107-117.

Wang, W., B. Lu, W. Dong and J. Li (2008). Multi-scale CFD simulation of operating diagram for gas-solid risers. *The Canadian Journal of Chemical Engineering* 82, 448-457.

Weber, J. M., K. J. Layfield, D. T. Van Essendelft and J. S. Mei (2013). Fluid bed characterization using Electrical Capacitance Volume Tomography (ECVT), compared to CPFD Software's Barracuda. *Powder Technology* 250, 138-146.

Wen, C. and Y. Yu (1966). Mechanics of fluidization, *Chemical Engineering Progress Symposium Series* 62 (1966) 100–111.

Werther, J. (2005). Fluid dynamics, temperature and concentration fields in large-scale CFB combustors, in: *Circulating Fluidized Bed Technology-VIII, Kefa, C., (Ed.),* International Academic Publishers, Beijing, pp. 1-25.

Xie, J., W. Zhong, Y. Shao, Q. Liu, L. Liu and G. Liu (2017). Simulation of Combustion of Municipal Solid Waste and Coal in an Industrial-Scale Circulating Fluidized Bed Boiler. *Energy Fuels* 31, 14248-14261.

Yang, N., W. Wang, W. Ge and J. Li (2003). CFD simulation of concurrent-up gas-solid flow in circulating fluidized beds with structure-dependent drag coefficient. *Chemical Engineering Journal* 96, 71-80

Yang, N., W. Wang, W. Ge, L. Wang, J. Li (2004). Simulation of Heterogeneous Structure in a Circulating Fluidized-Bed Riser by Combining the Two-Fluid Model with the EMMS Approach. *Industrial & Engineering Chemistry*

Research 43(18), 5548-5561.

Yeoh, G. H. and J. Tu (2009). *Computational Techniques for Multiphase Flows.* Butterworth-Heinemann.

Zeneli, M., A. Nikolopoulos, N. Nikolopoulos, P. Grammelis and E. Kakaras (2015). Application of an advanced coupled EMMS-TFM model to a pilot scale CFB carbonator. *Chemical Engineering Science* 138, 482-498.

Zhang, N., B. N. Lu, W. Wang and J. H. Li (2008). Virtual experimentation through 3D full-loop simulation of a circulating fluidized bed. *Particuology* 6, 529-539.

Zhang, N., B. N. Lu, W. Wang and J. H. Li (2010). 3D CFD simulation of hydrodynamics of a 150 MWe circulating fluidized bed boiler. *Chemical Engineering Journal* 162, 821-828.